The Impact of Carbon Support Catalyst from Lignin-Derived Phenolic in Ozonation Process

Budi Satria Panandita[1*], Lalak Tarbiyatun Nasyin Maleiva[1]
[1] Jurusan Teknik Kimia, Fakultas Teknik, Universitas Tanjungpura
Jl. Prof. Dr. H. Hadari Nawawi, Pontianak, Kalimantan Barat
[*]Email: Budisatriapanandita@teknik.untan.ac.id

Abstrak

Penelitian ini dimaksudkan untuk mengevaluasi efektivitas karbon pendukung katalis dari turunan fenol lignin pada proses oksidasi dengan ozon. *Methylene blue* dipilih sebagai model limbah cair. Performa proses ozon melalui model kinetika. Selain itu, suhu proses dipelajari pengaruhnya terhadap proses. Berdasarkan analisis N_2-soprtion didapat luas permukaan spesifik karbon pendukung adalah 36,16 m^2/g dengan rata-rata jari pori 1,58 nm. Karbon teremban Fe memperlihatkan efisiensi degradasi lebih dari 90% dalam 30 menit. Performa dari katalis dijelaskan dengan model *pseudo-first order* dan *non-linear kinetic*. berdasarkan parameter termodinamika menunjukkan reaksi oksidasi dengan ozon merupakan reaksi endotermis dan tidak spontan.

***Kata kunci**:* katalis karbon, *methylene Blue*, model kinetika, katalitik ozon, termodinamika

Abstract

The research described herein evaluated the effectiveness of a carbon-supported catalyst synthesized from lignin-derived phenol for ozonation, using methylene blue (MB) as a representative wastewater pollutant. The effectiveness of the degradation process was evaluated through kinetics. Furthermore, the effect of temperature on MB oxidation was investigated. The N_2-sorption analysis confirmed a specific surface area of the carbon support of 36.16 m^2/g, with a corresponding average pore radius of 1.58 nm. Fe-loaded carbon support achieves MB decolorization over 90% within 30 minutes. Pseudo-first-order and non-linear kinetic models described the catalyst's performance. The decolorization process was thermodynamically demonstrated to be endothermic and non-spontaneous.

***Keywords**: carbon catalyst, catalytic ozonation, methylene blue, kinetic model, thermodynamics*

1. INTRODUCTION

Recently, advanced oxidation processes (AOPs) have gained widespread acceptance due to their robust oxidative capabilities and broad applicability in wastewater treatment. AOPs emphasize the production of highly reactive oxidants that are capable of effectively degrading organic contaminants (Saravanan *et al.*, 2022). Ozon oxidation is considered one of the AOP techniques commonly employed for removing organic compounds by oxidation reaction with powerful, non-selective, and free of secondary pollutants (C. V. Rekhate and Srivastava, 2020; Ganiyu, Sable and El-din, 2022). Organic pollutants can be degraded by ozonation through direct and indirect pathways. In the direct pathway, pollutants are oxidized by ozone molecules, while the indirect pathway involves the interaction of pollutants with hydroxyl radicals (·OH), which transform into harmless byproducts like water and carbon dioxide (Malik *et al.*, 2020; P. Li *et al.*, 2024). Direct ozonation is relatively inefficient due to its high selectivity, given that efficient degradation was limited to aromatic compounds bearing nucleophilic functional groups or unsaturated aliphatic structures. whereas hydroxyl radicals were able to oxidize non-selectively toward a wide range of organic compounds. (Faria., 2008)(S. Zhang *et al.*, 2016).

However, ozone exhibited several limitations, particularly its relatively low solubility and stability in water. Therefore, catalytic ozonation using Fe-supported materials has been widely used to enhance the degradation of various contaminants (Wang and Bai). In several materials, carbon was used as a catalyst support due to its outstanding properties, such as high stability in aqueous media, low sensitivity to toxic and organic substances, large pore volume, and high thermal stability (Nasseh *et al.*, 2020). Among carbon material sources,

lignin is a plentiful, sustainable, and cost-effective aromatic biomass. Lignin as an eco-friendly solvent for producing carbon material through a two-step carbonization process. The macromolecular and basic structural units of lignin are similar to those of phenol (Gong *et al.*, 2022). Lignin contains abundant phenolic and aliphatic hydroxyl groups, enabling its use as an alternative precursor to phenol in phenol-formaldehyde resin synthesis. (Zeng *et al.*, 2020) (Li *et al.*, 2023). Therefore, lignin can be utilized to synthesize lignin-formaldehyde resins, which may subsequently be converted into polymer-derived carbon materials

In this experiment, methylene blue, as a simulated wastewater compound, was employed. The oxidation efficiency in aqueous solution with the carbon-supported catalyst was evaluated by kinetic analysis to determine reaction behavior and associated parameters. In addition, thermodynamic parameters were calculated to evaluate the influence of the temperature process.

2. METHODS

2.1 Materials

The catalyst oxidation employed in this research used polymer-derived carbon obtained by carbonizing phenol-derived lignin and formaldehyde. FeCl3·6H2O was used as the iron precursor for catalyst preparation. During the ozonation experiment, 95% methylene blue from Sigma-Aldrich was selected as the target pollutant, while ozone generated by an ozone generator was used as the source of hydroxyl radicals.

2.2 Catalyst preparations

The carbon-supported material was prepared via a two-step procedure, i.e., the synthesis of phenol-derived lignin formaldehyde and carbon conversion. The polymer precursor was composed of formaldehyde and phenol-derived lignin. The molar ratio of phenol-derived lignin and formaldehyde was fixed to 1 : 2.8. The mass fraction of catalyst was 1% of the total solution. Then, the polymer material was placed in the furnace and heated to 800 °C at a ramp rate of 5 °C. The furnace was cooled down to ambient temperature overnight.

2.3 Catalyst characterization

The pore characteristics of the carbon support were analyzed by N2 sorption. The multipoint Brunauer-Emmett-Teller (BET) method was used to evaluate the specific surface area using constant physical parameters. The total pore volume was assessed using the quantity of N_2 measured at the corresponding relative pressure, while the average pore radius was quantified using the Barrett-Joyner-Halenda (BJH) method.

2.4 Decolorization study

The MB oxidation was conducted in a batch system. All batch operations were carried out in a glass beaker at various temperatures (30, 40, and 50 °C). For each run, 10 mg L^{-1} MB in 50 mL of solution was introduced into the glass beaker and agitated at a constant speed. A 25 mg mass of catalyst was added. Samples were analyzed at wavelength 664 nm using a ultraviolet-visible (UV/Vis) spectrophotometer to monitor MB decolorization (Misran *et al*, 2018). The decolorization efficacy was calculated using Eq. 1.

$$\text{Percentage Removal (\%)} = \frac{A_0 - A_t}{A_0} \times 100\% \quad (1)$$

where A_0 is initial absorbance and A_t denoted absorbance at time t in minutes.

2.5 Reaction kinetics and thermodynamic study

The reaction kinetics were evaluated using a pseudo-first-order model, if the dissolved ozone concentration during the reaction remained constant and that the reaction occurs exclusively in the liquid phase. Therefore, MB oxidation by hydroxyl radicals can be described by several possible reaction mechanisms (Shang *et al.*, 2024). The concentration of hydroxyl radicals could not be measured directly. For the experimental conditions employed, the rate constant was considered independent of time. The first-order kinetic equation was described by Eq. 2.

$$-r = \frac{dC_{MB}}{dt} = kC_{MB} \quad (2)$$

Where C_A represents the MB concentration, and k denotes the first-order rate constant. The kinetics of oxidation were studied at different times (5 to 30 min) under varied temperatures. In compliance with the Lambert-Beer equation law, concentration is directly proportional to the absorbance (Giwa *et al.*, 2020). Consequently, Eq. 2 was rearranged into Eq. 3.

$$\ln\left(\frac{A_{MB}}{A_{MB_0}}\right) = -kt \qquad (3)$$

The rate constant (k) was determined from the slope of the color versus time plot. Nonlinear approaches were employed to describe the oxidation kinetics of the MB (Tirpanci *et al*, 2025). In this study, the kinetic data were fitted using an exponential decay function.

To evaluate the thermodynamic properties in terms of enthalpy, entropy, and Gibbs free energy, expressed in Eq. 4.

$$\ln k = \frac{E}{R}\left(\frac{1}{T}\right) + \ln A \qquad (4)$$

where T is the temperature (K), E represents the activation energy, A is the Arrhenius constant, and R denotes the universal gas constant. The energy changes were further studied using the Eyring-Polanyi general-form equation, which is similar to the Arrhenius equation, as expressed in Eq. 5.

$$k = \frac{k_B T}{h}\, e^{-\frac{\Delta G}{RT}} \qquad (5)$$

$$\Delta G = \Delta H - T\Delta S \qquad (6)$$

The Eyring-Polanyi Linear Form Equation was given in Eq. 7.

$$\ln\left(\frac{k}{T}\right) = \frac{-\Delta H}{R}\frac{1}{T} + \ln\left(\frac{k_B}{h}\right) + \frac{\Delta S}{R} \qquad (7)$$

The plot $\ln\frac{k}{T}$ vs 1/T showing slope $\frac{\Delta H}{R}$ for the determined activation enthalpy. The intercept was used to calculate activation entropy, and the activation of Gibbs free energy was estimated using Eq. 6.

3. RESULTS AND DISCUSSIONS

3.1 Carbon Support Pore Structure

The pore structure was considered a key factor in determining catalytic performance. The characterization of the carbon support using N2 Sorption is illustrated in Fig. 1. The results indicated that the carbon support exhibited predominantly micropore characteristics, with pore sizes of 0.7 and 0.83 nm. In addition, the mesopore was observed with a pore size of 2.4 nm. The summary of pore structural properties is presented in Table 1. The N2 adsorption capacity indicated that the specific surface area of the carbon support is 36.16 m2/g, with an average pore radius of 1.58 nm. A small surface area of carbon support may be caused by large pores and wider distances between pore walls. Consequently, the total internal surface area decreases (Z. Li *et al.*, 2024). Overall, the porosity analysis revealed that the carbon material has a wide range of pore sizes, indicating it is appropriate for evaluating the kinetic effect of porosity on MB degradation.

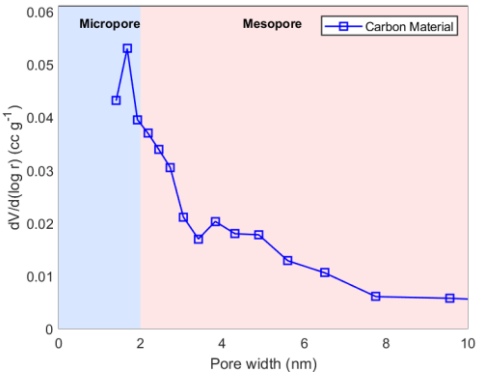

Fig. 1. Pore size distribution curves for carbon support material.

Table 1. Properties of Carbon support

Sample	Specific surface area (SSA) [m²/gram]	Total pore volume [cm³/gram]	Average Pore Radius [nm]
Carbon support	36.1604	2.874 x 10^{-2}	1.5899

3.2 Catalytic Performance

The effectiveness of both ozonation and catalytic ozonation for MB oxidation was assessed using an iron-loaded carbon-supported catalyst. As shown in Fig. 2, the rapid oxidation reaction of MB occurred in the aqueous solution. Overall, catalytic ozonation exhibited higher removal than ozonation. The oxidation process was primarily attributed to hydroxyl radicals generated by ozone decomposition. The presence of an iron catalyst enhanced hydroxyl radical production, as Fe sites on

the catalyst surface promoted ozone adsorption and facilitated ozone activation and decomposition, thereby increasing the production rate of hydroxyl radicals (Van *et al.*, 2019). Nevertheless, both processes achieved more than 90% decolorization of MB, with or without a catalyst, after 30 minutes of reaction. Indicating no substantial difference in the final removal efficiency. However, the catalytic ozonation process showed a higher decolorization rate compared to the non-catalytic ozonation system

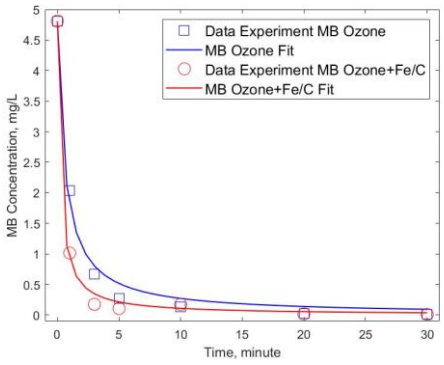

Fig. 2. Concentration profile of methylene blue

3.3 Decolorization kinetics

The kinetics of dye decolorization during O_3 process were investigated at various contact times and temperatures. The rate constant (k) was derived from the kinetic data by applying a pseudo-first-order kinetic model to determine the decomposition of the MB dye. The data obtained were presented in Table 2, however, the experimental data did not exhibit an adequate fit to the first-order kinetic model for any of the MB tests conducted in this study (Fig 3a). The first-order reaction rate constant for MB degradation often varies by many orders of magnitude due to the presence of a highly ozone-reactive group. Overall, MB kinetics were influenced by a multi-reaction radical hydroxyl mechanism (S Zhang *et al.*, 2016).

The non-linear model (exponential decay) in Fig. 3b was tested. The non-linear model shows an initial rapid reaction due to high reactivity with O3, and the high k value leads to a quick breakdown. Catalytic ozonation has the highest k compared with the single ozone process at any temperature. The initial rapid oxidation is likely due to ozone's high reactivity. The low oxidation may be caused by limited MB availability and formation of reactive byproduct (Tirpanci *et al*, 2025). However, in this study, the nonlinear model provides simpler, more reliable data without the complexity of the parameter model, enhancing its predictive applications.

Table 2. Rate parameters for Methylene Blue decolorization

Variation	Pseudo-first order model		Exponential decay model		
	k_1	R^2	k_2	R^2	RMSE
Fe/C	0.1370	0.84	1.6226	0.99	0.0732
30 ºC	0.1357	0.92	0.6665	0.97	0.1259
40 ºC	0.1338	0.79	0.8375	0.99	0.0650
50 ºC	0.1743	0.75	0.8272	0.99	0.1324

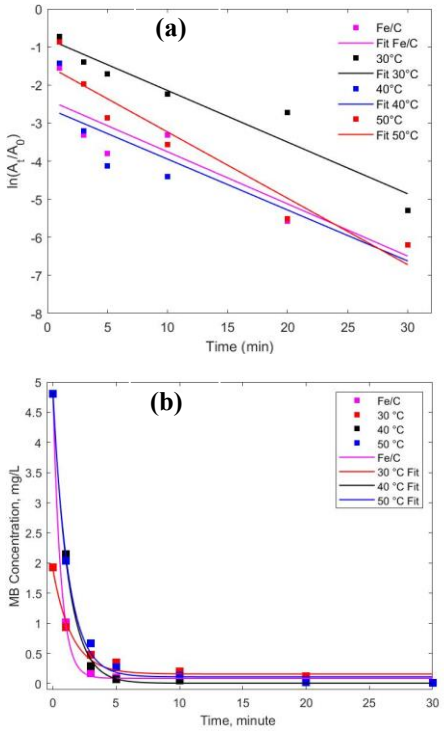

Fig. 3 Kinetic model for degradation of Methylene Blue, plots of pseudo first-order (a) exponential decay model (b)

3.4 Thermodynamics Studies

The thermodynamic parameters, such as enthalpy, entropy, and Gibbs free energy, and activation parameters were computed from the Eyring-Polanyi plot. The activation energy was calculated from the slope of the Arrhenius plot in Fig. 4a to be 8.609 kJ/mol. The result indicated that the ozone reaction has a low energy requirement. The enthalpy and entropy were determined from the Eyring-Polanyi plot in Figure 4b. The calculated enthalpy was 6.05 kJ/mol. The

observed positive value demonstrates that the oxidative reaction was endothermic. The measured activation entropy was -227.66 J/mol. Entropy value reflects the system's degree of disorder (Wen *et al.*, 2021). Gibbs' free energy was computed from the enthalpy and entropy values at various temperatures. The values were determined to be 73.89, 76.17, and 78.45 kJ/mol. The retention of positive numbers indicated that the reaction is thermodynamically non-spontaneous (Londero *et al.*, 2025).

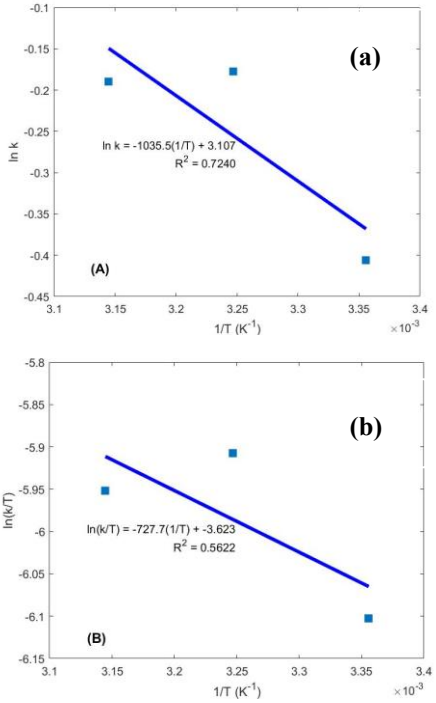

Fig. 4 Plots of oxidation of MB (a) ln k vs 1/T and (b) ln (k/T) vs 1/T

4 CONCLUSION

The influence of process parameters on MB oxidation in the presence of the carbon-supported catalyst was investigated. Ozonation was evaluated using UV/Vis measurements. It has been demonstrated that Fe-supported carbon in the ozonation process can degrade MB with efficiency above 90% under aqueous ozone treatment. The kinetics of dye decolorization at variable contact durations from 5 to 30 minutes via the O_3 process were examined, revealing the rapid oxidation that was best fit by the non-linear model (exponential decay model). Thermodynamic analysis revealed that the oxidative ozonation was endothermic and non-spontaneous.

REFERENCE

Faria, P.C.C., (2008). '*Catalytic ozonation of sulfonated aromatic compounds in the presence of activated carbon*'. Applied Catalysis B: Environmental Vol. 83 (1-2), pp. 150–159. Available at: https://doi.org/10.1016/j.apcatb.2008.02.010

Ganiyu, S.O., Sable, S. and El-din, M.G. (2022) '*Advanced oxidation processes for the degradation of dissolved organics in produced water : A review of process performance, degradation kinetics and pathway*'. Chemical Engineering Journal. Vol. 429 (Feb 2021). p.132492. Available at: https://doi.org/10.1016/j.cej.2021.132492

Giwa, A.R.A. *et al.* (2020) 'Kinetic and thermodynamic studies of fenton oxidative decolorization of methylene blue', *Heliyon*, Vol. 6(8), pp. 4–10. Available at: https://doi.org/10.1016/j.heliyon.2020.e04454

Gong, X. *et al.* (2022) 'A Review on Lignin-Based Phenolic Resin Adhesive', *Macromolecular Chemistry and Physics*, Vol. 223(4) p.2100434. Available at: https://doi.org/10.1002/macp.202100434.

Li, P. *et al.* (2023) 'Preparation of spherical porous carbon from lignin-derived phenolic resin and its application in supercapacitor electrodes', *International Journal of Biological Macromolecules*, 252(Dec), p.126271. Available at: https://doi.org/10.1016/j.ijbiomac.2023.126271

Li, P. *et al.* (2024). '*Treatment of membrane-concentrated landfill leachate by heterogeneous chemical and electrical Fenton processes with Iron-loaded granular activated carbon catalysts*'. Journal of Environmental Chemical Engineering, Vol 12(2), p112337. Available at: https://doi.org/10.1016/j.jece.2024.112337

Li, Z. *et al.* (2024). '*Advanced fabrication of lignin-formaldehyde resin derived*

carbon microspheres via spray drying'. Ceramics International 50(19), pp. 34510–34518. Available at: https://doi.org/10.1016/j.ceramint.2024.05.340

Londero, M. *et al.* (2025). '*Catalytic ozonation for the efficient degradation of tetracycline using $CoFe_2O_4$@TiO_2 ceramic nanocomposite : Kinetic , thermodynamic and machine learning study*'. Ceramics International, Vol. 51(6), pp. 7143–7158. Available at: https://doi.org/10.1016/j.ceramint.2024.12.149

Malik, S.N. *et al.* (2020). '*Hybrid ozonation process for industrial wastewater treatment : Principles and applications : A review*'. Journal of Water Process Engineering 35(June 2020), p.101193. Available at: https://doi.org/10.1016/j.jwpe.2020.101193.

Misran, E. *et al.* (2018). '*Removal efficiency of methylene blue using activated carbon from waste banana stem : Study on pH influence Removal efficiency of methylene blue using activated carbon from waste banana stem : Study on pH influence*', Earth and Environmental Science, Vol. 122 (Nov 2017) pp. 0–6. Available at: https://doi.org/10.1088/1755-1315/122/1/012085

Nasseh, N. *et al.* (2020). '*Preparation of activated carbon@ZnO composite and its application as a novel catalyst in catalytic ozonation process for metronidazole degradation*'. Advanced Powder Technology, Vol. 31(2), pp. 875–885. Available at: https://doi.org/10.1016/j.apt.2019.12.006.

Rekhate, C. V. and Srivastava, J.K. (2020). '*Recent advances in ozone-based advanced oxidation processes for treatment of wastewater- A review*', Chemical Engineering Journal Advances, 3(Nov 2020) p.100031. Available at: https://doi.org/10.1016/j.ceja.2020.100031.

Saravanan, A. *et al.* (2022). '*Chemosphere A detailed review on advanced oxidation process in treatment of wastewater: Mechanism, challenges and future outlook*', Chemosphere, 308(part 3) p.136524. Available at: https://doi.org/10.1016/j.chemosphere.2022.136524

Shang, J. *et al.* (2024). '*Kinetics of catalytic ozonation of methylene blue in wastewater with Fe/Ce co-doped in attapulgite*', Desalination and Water Treatment, Vol.317(Jan 2024), p.100023. Available at: https://doi.org/10.1016/j.dwt.2024.100023

Tirpanci, G., Kasler, D. and Yousef, A. (2025). '*Ozone degradation of structurally distinct pesticides : A non-linear kinetic modeling approach*', Science of the Total Environment, Vol.1001(October 2025) p.180482. Available at: https://doi.org/10.1016/j.scitotenv.2025.180482

Van, H.T. *et al.* (2019). '*Using FeO-constituted iron slag wastes as heterogeneous catalyst for Fenton and ozonation processes to degrade Reactive Red 24 from aqueous solution*', Separation and Puri fi cation Technology, Vol. 224(Oct 2019), pp. 431–442. Available at: https://doi.org/10.1016/j.seppur.2019.05.048

Wang, J. and Bai, Z. (2017) '*Fe-based catalysts for heterogeneous catalytic ozonation of emerging contaminants in water and wastewater*', Chemical Engineering Journal, Vol.312(March 2017), pp. 79–98. Available at: https://doi.org/10.1016/j.cej.2016.11.118

Wen, Y. *et al.* (2021) 'Pyrolysis of raw and anaerobically digested organic fractions of municipal solid waste: Kinetics, thermodynamics, and product characterization', *Chemical Engineering Journal*, 415(November 2020). Available at: https://doi.org/10.1016/j.cej.2021.129064.

Zeng, J. *et al.* (2020). '*Controllable depolymerization of lignin using carbocatalyst graphene oxide under mild conditions*', Fuel, Vol. 267(may 2020). p.117100. Available at: https://doi.org/10.1016/j.fuel.2020.117100

Zhang, S. *et al.* (2016). '*Evaluation of hydroxyl radical pathway and kinetic process for bubbling ozonation of methylene blue as*

reference compound', Desalination and Water Treatment, 57(23), pp. 10616–10625. Available at: https://doi.org/10.1080/19443994.2015.1038592